Susceptibility and surface magnetostatic modes for the spiral and cone states of rare-earth magnets

N. S. Almeida
Departamento de Física, Universidade Federal do Rio Grande do Norte, 59702 Natal, Rio Grande do Norte, Brazil

D. R. Tilley
Department of Physics, University of Essex, Colchester CO4 3SQ, United Kingdom
(Received 9 July 1990; revised manuscript received 25 October 1990)

Spiral states (in which the equilibrium spin vector rotates uniformly at right angles to a helical axis) and cone states (in which the spin vector rotates at an angle $\theta \neq 90°$ to the helical axis) are observed in various rare-earth magnets within some temperature interval. The spin-wave spectrum $\omega(\mathbf{k})$ is rederived, and the magnetic-susceptibility tensor is found, for the cone state; expressions for the spiral state are given as special cases. In the cone state, the susceptibility tensor has a gyromagnetic form, and has poles at the spin-wave frequencies $\omega(\pm\mathbf{k}_0)$, where $\mathbf{k}_0$ is the wave vector of the equilibrium helix; in the spiral state, the susceptibility tensor is diagonal, with a single pole at $\omega(\mathbf{k}_0)$, since the frequencies $\omega(\pm\mathbf{k}_0)$ are degenerate in the spiral. The results are applied to a calculation of the magnetostatic-surface-mode spectrum for the geometry in which the helical axis lies in the surface. In the cone state, propagation is nonreciprocal, but due to the existence of two poles, two surface-mode branches occur, with different ranges of allowed propagation directions; in the spiral state, propagation is reciprocal. The implications of the results for Brillouin scattering and attenuated total reflection are discussed, and a wide range of possible extensions of the calculations is outlined.

I. INTRODUCTION

Magnetism in rare-earth metals was the subject of intensive studies in the 1960s; the understanding achieved then has been summarized in a number of major reviews.[1-3] Interest in the subject is currently undergoing a revival as a result of the success in developing growth techniques for superlattices containing rare earths. Among the experimental techniques available for the investigation of such superlattices, Brillouin scattering by magnetostatic surface modes is expected to play a part.

Magnetostatic surface modes on a ferromagnet were investigated theoretically by Damon and Eshbach.[4] These modes were studied experimentally in the first instance by direct microwave excitation[5] and were later investigated much more comprehensively by Brillouin scattering. Extensive discussions of these results are available.[6-8] With the development of magnetic superlattices, both theoretical[7,9] and experimental[10] studies of magnetostatic modes in superlattices and the resulting light-scattering spectrum were carried out in quick succession.

Our purpose in this paper is to initiate a theoretical study of magnetostatic and related modes on the surfaces of rare-earth metals and of superlattices containing rare earths. The fundamental physical quantity for all such work is the susceptibility tensor describing the response of the magnetization in a rare-earth metal to a driving magnetic field at microwave or far-infrared frequency, and the central part of this paper is therefore the evaluation of the susceptibility tensor. The rare earths display a rich variety of magnetic ordering;[1] apart from simple ferromagnetic alignment, observed in Gd, and in Tb and Dy at low temperatures, two of the most important—the ones with which we shall be concerned—are the spiral and cone states, the former occurring in Tb (221 K $< T <$ 230 K), in Dy (85 K $< T <$ 179 K), and in Ho (20 K $< T <$ 133 K), and the latter in Ho ($T <$ 20 K) and in Er ($T <$ 20 K).

Despite the variety of orderings, the rare earths have many features in common, and indeed they can all be described by the same phenomenological Hamiltonian.[2] The metals all order in the hexagonal-close-packed (hcp) structure, and in all the various states the spins within a given close-packed plane are aligned ferromagnetically. In the spiral state, the moment lies in the plane, with its orientation advancing by ϕ from one plane to the next. In the cone state, the moment is lifted out of the plane and makes an angle θ with the normal (z axis); the projection in the x-y plane advances by ϕ between planes. This means that the Hamiltonian can be taken as one dimensional, with effective exchange constants between different planes. The exchange derives from the Ruderman-Kittel-Kasuya-Yosida (RKKY) interaction and is therefore relatively long ranged and can oscillate in sign. For a general description it is sufficient to use an effective Hamiltonian with nearest- and next-nearest-neighbor exchange. If the former is ferromagnetic and the latter antiferromagnetic in sign, then a spiral state can result from competition between the two signs of exchange.[11]

In addition to the exchange interactions, anisotropy terms may be included. While an anisotropic exchange can be introduced, it is sufficient for our present purposes to use single-ion anisotropy terms. For the spiral state,

we include only a term KS_z^2, which ensures that the spins remain within the close-packed planes, while for the cone states at least a term LS_z^4 is needed in order to ensure a cone angle $\theta < 90°$. A possible term in S_z^6 and in-plane anisotropy terms are omitted: the former would not alter the results in any significant way; implications of omitting the latter are discussed in Sec. VI. Finally, magnetostrictive effects are important, particularly in determining the phase transitions between different ordered states and the temperature dependence of parameters like the angles θ and ϕ. They can be included implicitly, to some extent, if the exchange parameters are taken to have a temperature dependence consistent with the known temperature dependence of θ and ϕ.

The plan of the paper is as follows. In Sec. II we derive the equilibrium values of θ and ϕ. In Sec. III we give the equations of motion for the spin-deviation operators within the semiclassical approximation; the derivation is equivalent to that in the original literature,[1-3] but it is given in a modified form that is more suitable for the tasks at hand. The spin-wave dispersion relation is derived from the equations of motion and illustrated numerically. Both the equations of motion and dispersion relation are given for the cone state since the spiral state is simply the special case $\theta = 90°$. The susceptibility tensor is derived in Sec. IV. In Sec. V we give some elementary applications of the susceptibility tensor, namely, the magnetostatic modes on semi-infinite and finite-slab specimens in the cone and spiral states. Conclusions and a general discussion are presented in Sec. VI.

II. EFFECTIVE HAMILTONIAN AND EQUILIBRIUM STATES

The Hamiltonian is taken as

$$\mathcal{H} = -J_1 \sum_n \mathbf{S}_n \cdot \mathbf{S}_{n+1} + J_2 \sum_n \mathbf{S}_n \cdot \mathbf{S}_{n+2} + \sum_n (KS_{nz}^2 + LS_{nz}^4) - \gamma H_0 \sum_n S_{nz} - \gamma \mathbf{h} \cdot \sum_n \mathbf{S}_n \ , \tag{1}$$

where the sums are over close-packed planes labeled n. The exchange and anisotropy terms were discussed in Sec. I; in much of the early literature, the Hamiltonian is often expressed as an unrestricted sum over neighbors i and j, so that the values of J_1 and J_2 appearing in (1) are twice those in those papers. Equation (1) includes a static external field $\mathbf{H}_0$ in the z direction (normal to the close-packed planes); as will be mentioned in Sec. VI, an external field in the x-y plane leads to more subtle effects and is not included. The last term in (1) is the interaction with an rf (microwave or infrared) applied field $\mathbf{h}$; the susceptibility is the linear response of the magnetization to $\mathbf{h}$.

The equilibrium configuration is assumed to take the form

$$\mathbf{S} = S(\sin\theta\cos(n\phi), \sin\theta\sin(n\phi), \cos\theta) \ , \tag{2}$$

where S stands for the total angular momentum J.[1] This form is substituted into (1) (without the final term), and the resulting energy $E(\theta,\phi)$ is minimized with respect to θ and ϕ (the justification for minimizing the internal energy rather than the free energy is discussed in Ref. 1). Minimization with respect to ϕ yields

$$\cos\phi = J_1/4J_2 \ , \tag{3}$$

so that the cone (or spiral) state is energetically favorable, provided that the nearest- and next-nearest-neighbor exchange interactions are, respectively, ferromagnetic and antiferromagnetic, as indicated by the signs in (1) and provided that $J_2 > J_1/4$. Minimization with respect to θ gives

$$4LS^3\cos^3\theta + 2S(2J_2 - J_1 + J_1^2/8J_2 + K)\cos\theta - \gamma H_0 = 0 \ . \tag{4}$$

III. EQUATIONS OF MOTION AND SPIN-WAVE DISPERSION

Equations of motion for the spin operators at site n may be derived from (1) in the usual way. Within the usual semiclassical approximation, we linearize them by defining

$$\mathbf{S}_n = S(\mathbf{A}_n + \boldsymbol{\alpha}_n) \ , \tag{5}$$

where $\mathbf{A}_n$ is the unit vector appearing in (2). We retain only terms linear in $\boldsymbol{\alpha}_n$ or $\mathbf{h}$ and define $\alpha_n^{\pm} = \alpha_n^x \pm i\alpha_n^y$, $h^{\pm} = h^x \pm ih^y$. The linearized equations of motion are

$$\dot{\alpha}_n^{\pm} = \mp iG_0\alpha_n^{\pm} \pm i\Omega(k_0)\sin\theta\exp(\pm in\phi)\alpha_n^z \pm i(\Omega_A + 3\Omega_L\cos^2\theta)\exp(\pm in\phi)\alpha_n^z$$
$$\mp i\sin\theta\exp(\pm in\phi)[\Omega_1(\alpha_{n+1}^z + \alpha_{n-1}^z) - \Omega_2(\alpha_{n+2}^z + \alpha_{n-2}^z)]$$
$$\pm i\cos\theta[\Omega_1(\alpha_{n+1}^{\pm} + \alpha_{n-1}^{\pm}) - \Omega_2(\alpha_{n+2}^{\pm} + \alpha_{n-2}^{\pm})] \pm i\gamma\cos\theta h^{\pm} \mp i\gamma\sin\theta\exp(\pm in\phi)h^z \ , \tag{6}$$

$$\dot{\alpha}_n^z = \tfrac{1}{2}i\Omega(k_0)\sin\theta[\alpha_n^+\exp(-in\phi) - \alpha_n^-\exp(in\phi)] - \tfrac{1}{2}i\Omega_1\sin\theta[(\alpha_{n+1}^+ + \alpha_{n-1}^+)\exp(-in\phi) - (\alpha_{n+1}^- + \alpha_{n-1}^-)\exp(in\phi)]$$
$$+ \tfrac{1}{2}i\Omega_2\sin\theta[(\alpha_{n+2}^+ + \alpha_{n-2}^+)\exp(-in\phi) - (\alpha_{n+2}^- + \alpha_{n-2}^-)\exp(in\phi)] - \tfrac{1}{2}i\gamma\sin\theta[h^+\exp(-in\phi) - h^-\exp(in\phi)] \ , \tag{7}$$

where

$$\Omega_A = 2KS \ , \tag{8}$$

$$\Omega_L = 4LS^3 \ , \tag{9}$$

$$\Omega_1 = J_1 S \ , \tag{10}$$

$$\Omega_2 = J_2 S \ , \tag{11}$$

$$G_0 = (2\Omega_1 - 2\Omega_2 - \Omega_A)\cos\theta - \Omega_L \cos^3\theta + \gamma \mathbf{H}_0 \ . \tag{12}$$

The function $\Omega(q)$ is defined for general q by

$$\Omega(q) = 2\Omega_1 \cos(\tfrac{1}{2}qc) - 2\Omega_2 \cos(qc) \ , \tag{13}$$

where c is the length of the crystallographic c axis so that $\frac{1}{2}c$ is the distance between close-packed planes; $\Omega(q)$ is proportional to the Fourier transform of the exchange interaction. k_0 is defined as the wave number of the equilibrium configuration, so that

$$\tfrac{1}{2}k_0 c = \phi \ . \tag{14}$$

It can be seen that with these definitions, (4) can be written as

$$G_0 = \Omega(k_0)\cos\theta \ . \tag{15}$$

The equations of motion for α_n^+, α_n^-, and α_n^z are not all independent; it is to be expected from (5) that $\dot{\boldsymbol{\alpha}}_n$ and $\mathbf{A}_n$ are orthogonal, and $\mathbf{A}_n \cdot \dot{\boldsymbol{\alpha}}_n = \mathbf{0}$, so that

$$\sin\theta[\dot{\alpha}_n^+ \exp(-in\phi) + \dot{\alpha}_n^- \exp(in\phi)] + 2\cos\theta \dot{\alpha}_n^z = 0 \ . \tag{16}$$

This is readily verified with the use of (15).

Equation (16) can be used to eliminate α_n^-, for example. In the resulting equations, it is convenient to define

$$\beta_n = \alpha_n^+ \exp(-in\phi) \ . \tag{17}$$

The coupled equations for β_n and α_n^z are then found to be

$$\begin{aligned}\dot{\beta}_n = {} & -i\Omega(k_0)\cos\theta\beta_n + i[\Omega(k_0) + \Omega_A + 3\Omega_L \cos^2\theta]\sin\theta\alpha_n^z - i\sin\theta[\Omega_1(\alpha_{n+1}^z + \alpha_{n-1}^z) - \Omega_2(\alpha_{n+2}^z + \alpha_{n-2}^z)] \\ & + i\cos\theta\{\Omega_1[\beta_{n+1}\exp(i\phi) + \beta_{n-1}\exp(-i\phi)] - \Omega_2[\beta_{n+2}\exp(2i\phi) + \beta_{n-2}\exp(-2i\phi)]\} \\ & + i\gamma\cos\theta h^+ \exp(-in\phi) - i\gamma\sin\theta h^z \ ,\end{aligned} \tag{18}$$

$$\begin{aligned}\dot{\alpha}_n^z = {} & i\Omega(k_0)\sin\theta\beta_n + i\Omega(k_0)\cos\theta\alpha_n^z - i\Omega_1\sin\theta\cos\phi(\beta_{n+1} + \beta_{n-1}) + i\Omega_2\sin\theta\cos 2\phi(\beta_{n+2} + \beta_{n-2}) \\ & - i\Omega_1\cos\theta[\alpha_{n-1}^z\exp(i\phi) + \alpha_{n+1}^z\exp(-i\phi)] - i\Omega_2\cos\theta[\alpha_{n-2}^z\exp(2i\phi) + \alpha_{n+2}^z\exp(-2i\phi)] \\ & - \tfrac{1}{2}i\gamma\sin\theta[h^+\exp(-in\phi) - h^-\exp(in\phi)] \ .\end{aligned} \tag{19}$$

The equations of motion for the spiral state are the special cases of (18) and (19) with $\sin\theta = 1$ and $\cos\theta = 0$; it is seen that this leads to a considerable simplification.

Equations (18) and (19) can be used for the derivation of both the spin-wave dispersion equation and the susceptibility tensor. For the former, we solve the homogeneous equations with $\mathbf{h} = \mathbf{0}$ by means of the ansatz

$$\beta_n = \beta_0 \exp(iqz_n)\exp(-i\omega t) \ , \tag{20}$$

$$\alpha_n^z = \alpha_0 \exp(iqz_n)\exp(-i\omega t) \ , \tag{21}$$

where $z_n = \frac{1}{2}nc$ is the coordinate of the nth close-packed plane. This leads to the dispersion relation

$$\begin{aligned}\omega^2 + \omega\cos\theta[\Omega(k_0+q) - \Omega(k_0-q)] - \cos^2\theta[\Omega(k_0) - \Omega(k_0+q)][\Omega(k_0) - \Omega(k_0-q)] \\ - \sin^2\theta[\Omega(k_0) - \tfrac{1}{2}\Omega(k_0+q) - \tfrac{1}{2}\Omega(k_0-q)][\Omega(k_0) - \Omega(q) + \Omega_A + 3\Omega_L\cos^2\theta] = 0 \ .\end{aligned} \tag{22}$$

It is worth writing down the special case of the spiral explicitly:

$$\omega^2 = [\Omega(k_0) - \tfrac{1}{2}\Omega(k_0+q) - \tfrac{1}{2}\Omega(k_0-q)][\Omega(k_0) - \Omega(q) + \Omega_A] \ . \tag{23}$$

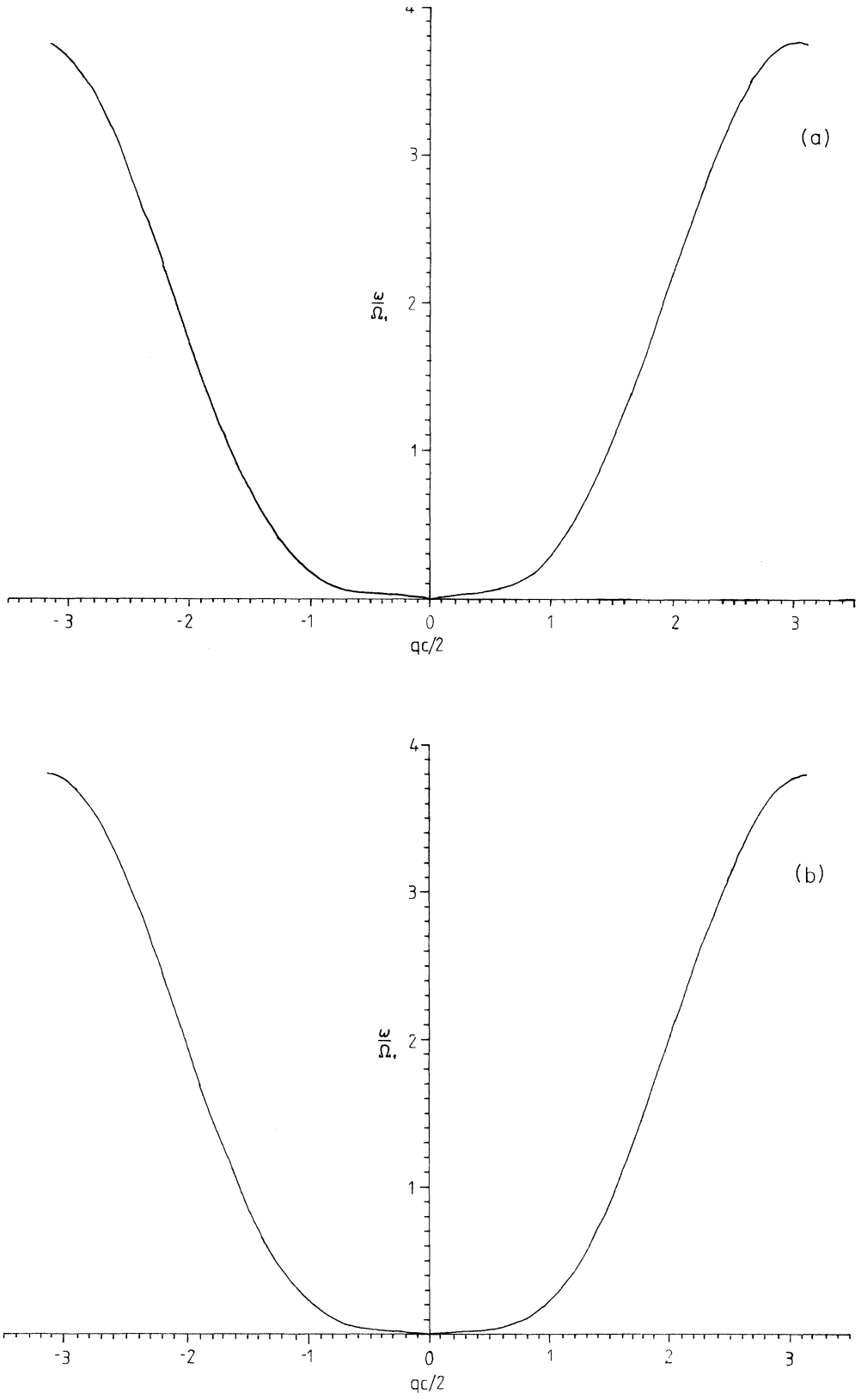

FIG. 1. Spin-wave dispersion curves for (a) cone state $\phi=30°$ and $\theta=80°$, corresponding to Ho at 20 K, and (b) spiral state $\phi=26.5°$ and $\theta=90°$, corresponding to Dy at 90 K.

Equation (22) is identical to that derived by Kaplan;[12] in making a comparison, it must be noted that he uses the $\exp(+i\omega t)$ frequency convention. Equation (22), unlike (23), had the property that $\omega(-q)\neq\omega(q)$. In fact, the equation for $\omega(-q)$ differs from that for $\omega(q)$ only by having the sign of the term linear in ω reversed, so that if the two roots of (22) are written $\omega_1(q)$ and $\omega_2(q)$, then $\omega_1(-q)=-\omega_1(q)$ and $\omega_2(-q)=-\omega_2(q)$. Since it is a condition of stability that one spin-wave frequency should be positive for each value of q, we may conclude that $\omega_1(q)$ (say) is positive and $\omega_2(q)$ is negative, and the physical spin-wave frequencies are $\omega(q)=\omega_1(q)$ and $\omega(-q)=-\omega_2(q)$.

Equations (22) and (23) are illustrated in Fig. 1. The numerical parameters required were determined as follows. Ω_2/Ω_1 was found from ϕ by means of (3); Ω_L/Ω_A was assigned the typical value of 0.1; Ω_1/Ω_A was found from (4). As required by (22) and (23), Fig. 1(b) is symmetric, $\omega(-q)=\omega(q)$, while Fig. 1(a) is asymmetric, although the asymmetry is not very marked for the cone angle $\theta=80°$.

IV. SUSCEPTIBILITY

As mentioned, the magnetic susceptibility tensor is proportional to the tensor giving the linear response of $\boldsymbol{\alpha}$ to $\mathbf{h}$. The frequency region of interest is where the spin-wave frequencies occur, that is, the microwave or far-infrared, and here the electromagnetic wavelength λ is much larger than the spiral period, $\lambda k_0 \gg 1$. It is therefore sufficient to take $\mathbf{h}$ spatially uniform, $\mathbf{h}\propto\exp(-i\omega t)$. We solve (18) and (19) for β_n and α_n^z, and it is convenient to take the components of $\mathbf{h}$ to be nonzero one at a time.

For $h^z\neq 0$, the solutions are of the form $\beta_n=\beta_0\exp(-i\omega t)$ and $\alpha_n^z=\alpha_0\exp(-i\omega t)$. When these are substituted into (19), the right-hand side vanishes, and so $\alpha_0=0$. Thus there is no longitudinal response, $\chi_{zz}=0$. Furthermore, although (18) gives a nonzero value of β_0, (17) and (16) show that α_n^+ and α_n^- contain the spatially varying terms $\exp(in\phi)$ and $\exp(-in\phi)$, respectively. These average to zero over any macroscopic volume of the crystal, and so there is no response of the magnetization components $M^{\pm}$ to h^z, $\chi_{\pm z}=0$. In all, then, $\chi_{iz}=0$.

For $h^+\neq 0$, the solutions take the form

$$\beta_n=\beta_0\exp(-in\phi)\exp(-i\omega t)$$

and

$$\alpha_n^z=\alpha_0\exp(-in\phi)\exp(-i\omega t)\ .$$

It follows from the second of these there is no response of M^z, $\chi_{z+}=0$, as indeed is necessary since χ must be Hermitian. Equation (17) shows that α_n^+ is spatially independent, $\alpha_n^+\propto\beta_0$, so that $\chi_{++}\neq 0$, but it follows from (16) that $\chi_{-+}=0$. The magnetic moment is $M^+=N\mu\alpha_n^+$, where N is the number of layers per unit volume and μ is the magnetic moment per layer. The solution of (18) and (19) for α_0 and β_0 then gives

$$\chi_{++}=-\gamma N\mu\{(\Omega_A+3\Omega_L\cos^2\theta)\sin^2\theta + [\omega+\Omega(k_0)\cos\theta - \Omega(2k_0)\cos\theta]\cos\theta\}/D_+\ , \quad (24)$$

where

$$D_+=[\omega+\Omega(0)\cos\theta-\Omega(k_0)\cos\theta] \times[\omega+\Omega(k_0)\cos\theta-\Omega(2k_0)\cos\theta] -[\Omega_A+3\Omega_L\cos^2\theta][\Omega(k_0)-\tfrac{1}{2}\Omega(0) -\tfrac{1}{2}\Omega(2k_0)]\sin^2\theta\ . \quad (25)$$

Comparison with the spin-wave dispersion equation (22) shows that $D_+=0$, and therefore χ_{++} has a pole at $\omega(-k_0)$, the frequency of the $q=-k_0$ spin wave.

A similar calculation to that just described gives

$$\chi_{--}=-\gamma N\mu\{\tfrac{1}{2}(\Omega_A+3\Omega_L\cos^2\theta)\sin^2\theta - [\omega-\Omega(k_0)\cos\theta + \Omega(2k_0)\cos\theta]\cos\theta\}/D_-\ , \quad (26)$$

where

$$D_-=[\omega-\Omega(0)\cos\theta+\Omega(k_0)\cos\theta] \times[\omega-\Omega(k_0)\cos\theta+\Omega(2k_0)\cos\theta] -[\Omega_A+3\Omega_L\cos^2\theta][\Omega(k_0)-\tfrac{1}{2}\Omega(0) -\tfrac{1}{2}\Omega(2k_0)]\sin^2\theta\ . \quad (27)$$

The tensor component χ_{--} has a pole at $\omega(k_0)$, the frequency of the $q=k_0$ spin wave.

We commented that (22) for the spin-wave frequencies has the property that the roots for $+q$ are $\omega(q)$ and $-\omega(-q)$. The denominators D_+ and D_- can therefore be written more concisely as

$$D_+=(\omega-\omega_-)(\omega+\omega_+)\ , \quad (28)$$

$$D_-=(\omega+\omega_-)(\omega-\omega_+)\ , \quad (29)$$

where

$$\omega_\pm=\omega(\pm k_0)\ . \quad (30)$$

Since the susceptibility tensor is diagonal in the $+,-,z$ frame, it takes the standard gyromagnetic form in the x,y,z frame, namely,

$$\begin{bmatrix} M_x \\ M_y \end{bmatrix} = \begin{bmatrix} \chi_a & i\chi_b \\ -i\chi_b & \chi_a \end{bmatrix} \begin{bmatrix} h^x \\ h^y \end{bmatrix}\ , \quad (31)$$

where to bring out the essential features of the frequency dispersion due to the poles we write

$$\chi_a=\frac{1}{2}\left[\frac{A_+}{(\omega-\omega_-)(\omega+\omega_+)}+\frac{A_-}{(\omega+\omega_-)(\omega-\omega_+)}\right]\ , \quad (32)$$

$$\chi_b=\frac{1}{2}\left[\frac{A_+}{(\omega-\omega_-)(\omega+\omega_+)}-\frac{A_-}{(\omega+\omega_-)(\omega-\omega_+)}\right] \quad (33)$$

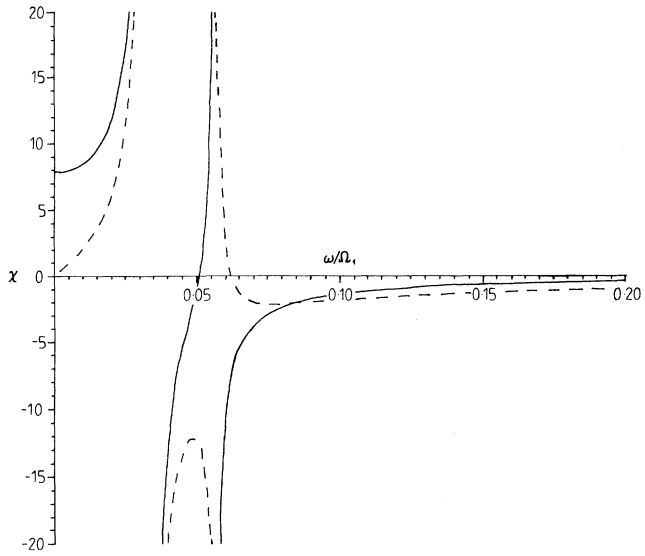

FIG. 2. Susceptibility-tensor components χ_a (——) and χ_b (— — —) for the cone state with $\phi=30°$ and $\theta=80°$, corresponding to the dispersion curve shown in Fig. 1(a).

Here A_+ and A_- are slowly varying functions of frequency.

Again, it is worth quoting the susceptibility tensor explicitly for the special case of the spiral state. As illustrated in Fig. 1, the resonance frequencies ω_+ and ω_- then coincide, as do the susceptibility components χ_{++} and χ_{--}:

$$\chi_{++}=\chi_{--}=\chi=-\tfrac{1}{2}\gamma N\mu\Omega_A/(\omega^2-\omega_R^2)\ , \tag{34}$$

with

$$\omega_R^2=\Omega_A[\Omega(k_0)-\tfrac{1}{2}\Omega(2k_0)-\tfrac{1}{2}\Omega(0)]\ , \tag{35}$$

the spin-wave frequency for $q=k_0$. It follows from (34) that, in the x,y,z frame,

$$\begin{bmatrix} M_x \\ M_y \end{bmatrix}=\begin{bmatrix} \frac{1}{2}\chi & 0 \\ 0 & \frac{1}{2}\chi \end{bmatrix}\begin{bmatrix} h^x \\ h^y \end{bmatrix}\ . \tag{36}$$

This is a similar diagonal form to that found for a uniaxial antiferromagnet in the absence of an applied static field.[7,13]

An example of the frequency dependence of the cone-state susceptibility-tensor components χ_a and χ_b is shown in Fig. 2; the parameters θ and ϕ are those used for the dispersion curve of Fig. 1(a). As was seen, that curve is asymmetric, $\omega(-q)\neq\omega(q)$, and consequently the two frequencies ω_+ and ω_- of (30) are different. This means, from (32) and (33), that χ_a and χ_b each have two distinct poles at ω_- and ω_+. Furthermore, the residues have the same sign at ω_- and opposite signs at ω_+. These properties are seen in Fig. 2. Decreasing the cone angle θ increases the asymmetry of the spin-wave dispersion curve, and therefore increases the separation of the resonance frequencies ω_- and ω_+, while increasing the

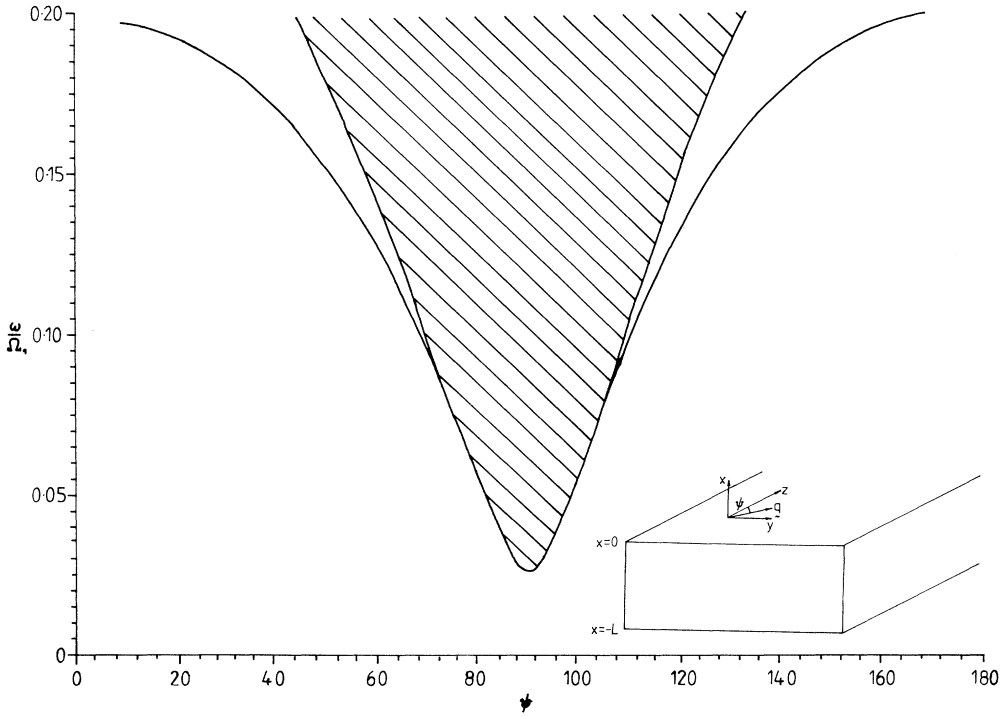

FIG. 3. Bulk-continuum regions (shaded) and surface-mode dispersion curve for the spiral state with $\phi=26.5°$. The frequency ω is scaled in terms of the exchange frequency Ω_1, defined in (10). Inset shows the notation. z is the helix axis; ψ is the angle between the helix axis and the propagation direction $\mathbf{q}$.

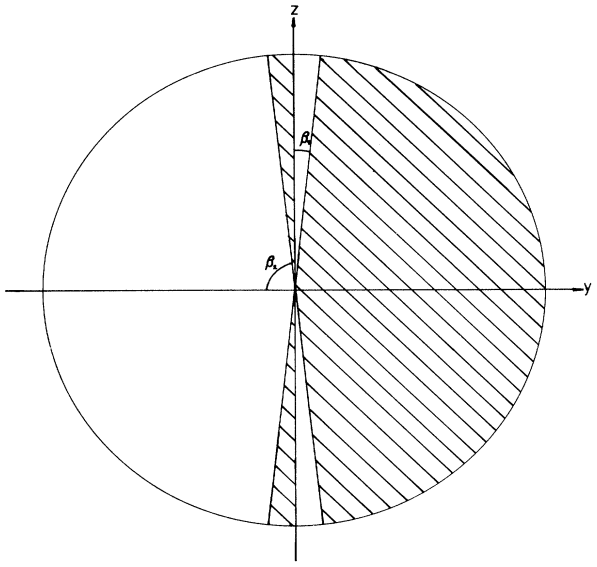

FIG. 4. Allowed directions of surface-magnetostatic-mode propagation (shaded) for the cone state. For the parameters used for the spin-wave dispersion curve [Fig. 2(a)], the angles are $\beta_1=5.8°$ and $\beta_2=83.7°$.

turn angle ϕ increases both ω_- and ω_+.

The spiral state is the special case of the cone when $\theta=90°$. In this case, the spin-wave dispersion curve [Fig. 1(b)] is symmetric; consequently ω_- and ω_+ coincide, and furthermore the off-diagonal component χ_b vanishes, so that the susceptibility tensor takes the diagonal form (36) in the x,y,z frame. The one-pole behavior of the single component χ is similar to that found in a uniaxial antiferromagnet; χ is positive for small frequency and negative for large frequency, with a pole at the resonance frequency ω_R and $\chi\to 0$ as $\omega\to\infty$. An increase of ϕ leads to an increase of the resonance frequency, as might be expected since the ordering is then becoming more antiferromagnetic in character.

V. MAGNETOSTATIC SLAB AND SURFACES MODES

The derivation of the dispersion equation for magnetostatic modes is well known,[7,8] and so we need only quote the results. We consider a finite slab extending from $x=-L$ to 0, with the z axis parallel to the surface, as shown in the inset of Fig. 3. For a given in-plane wave vector $\mathbf{q}_\parallel=(q_y,q_z)$, the normal component q_x is determined by

$$(1+\chi_a)(q_\parallel^2+q_x^2)-\chi_a q_z^2=0\ . \tag{37}$$

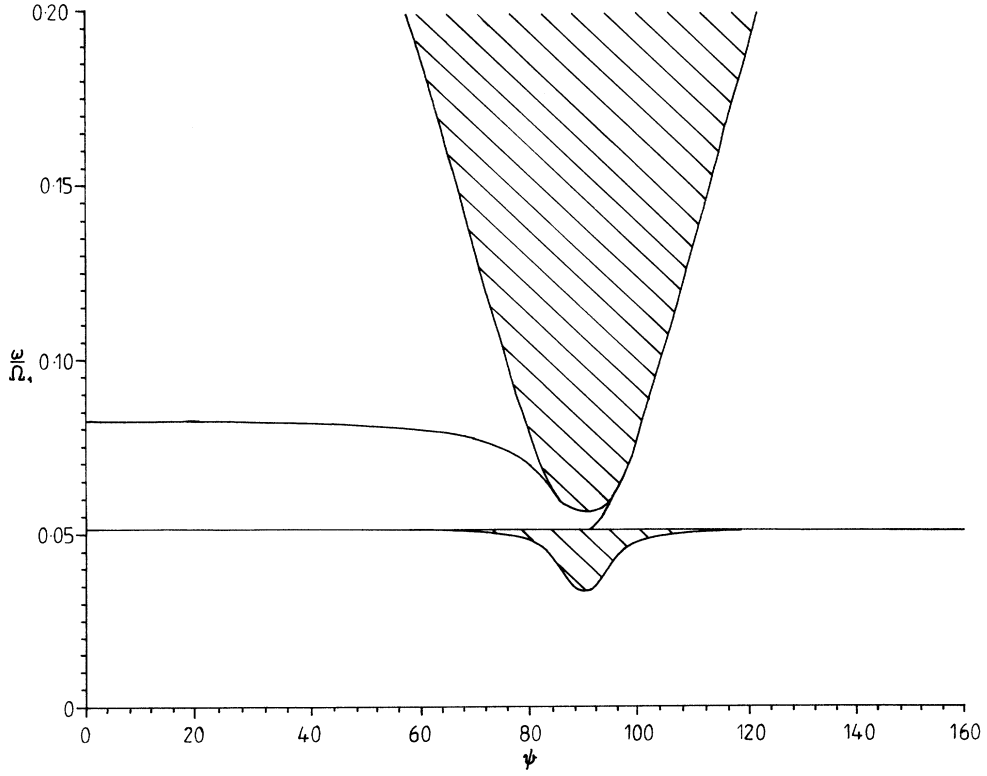

FIG. 5. Bulk-continuum regions (shaded) and surface-mode dispersion curves for the cone state with $\phi=30°$ and $\theta=80°$. Angle ψ defined in Fig. 3.

It can be real, corresponding to guided waves, or imaginary, corresponding to surface-type waves. Application of the boundary conditions at the surfaces of the slab gives

$$q_{\parallel}^2+2q_{\parallel}q_x(1+\chi_a)\cot(q_xL)-q_x^2(1+\chi_a)^2-q_y^2\chi_b^2=0\ . \tag{38}$$

Equations (37) and (38) determine the dispersion curves of the magnetostatic modes.

We illustrate these results with dispersion curves for semi-infinite specimens. Figure 3 shows the surface magnetostatic mode for the spiral state, which has the diagonal susceptibility tensor (36). It is seen that since χ is diagonal, the curve is symmetric about 90°; i.e., the $+z$ and $-z$ directions are equivalent. The value of the exchange constant J_1 in Dy is around 170 K,[1] i.e., 120 cm^{-1}, and so the ordinate in Fig. 3 is on a scale of order 10–20 cm^{-1}.

For the cone state, the $+z$ and $-z$ directions are no longer equivalent, and the presence of the off-diagonal terms in (31) lead to nonreciprocal propagation.[7] It is well known that in the relatively simple case of the surface of a ferromagnet, propagation is only possible within a wedge of directions centered on the $+y$ axis. For the cone state, however, the allowed propagation directions consist of a wedge in the $+y$ direction, together with two $-y$ tails stretching back from the z axis, as depicted in Fig. 4. Actual dispersion curves for Ho are shown in Fig. 5. The presence of the two poles at ω_+ and ω_- in the susceptibility components (32) and (33) leads to the appearance of two bulk-continuum frequency bands. As is seen, the $+y$ mode, $\psi<90°$, which is the analog of that found in a ferromagnet, is in the frequency region of the upper bulk continuum, while the $-y$ mode is largely within the frequency gap between the two bulk-continuum regions.

VI. DISCUSSION

Our main result is the derivation of the susceptibility tensor [Eqs. (31)–(33)] for the cone state with that for the spiral state [Eq. (36)] emerging as a special case. The derivation is a conventional one based on spin-wave theory, with appropriate anisotropy terms included. As in many other spin-wave treatments,[1] magnetostriction was not included, since its main effect is probably to stabilize equilibrium configurations. Damping terms do not appear in (31)–(33), but could be inserted phenomenologically in the usual way by the replacements $\omega_{\pm}\rightarrow\omega_{\pm}-i\Gamma_{\pm}$. The magnetic resonance results[1] indicate that damping is significant, but a detailed treatment is probably best left until appropriate experimental results are available.

One of the fascinating features of rare-earth magnetism is the range of equilibrium states that can be induced by applied magnetic fields.[1] A strong field applied along the c axis to the spiral state induces a conelike state, thus presumably inducing nonreciprocity in the magnetostatic surface modes. A fairly small field applied in the a-b plane to either the spiral state or the cone state distorts the uniform pitch of the helix, since the Zeeman energy favors orientation of the spins with a large component along the field direction. For fields which are still quite modest, of order 1 T in Dy,[1] the spiral flops to a fan state in which the spin directions simply oscillate about the magnetic field. An important extension of the present work would be the calculation of the susceptibilities and related properties in these field-distorted phases.

Starting some 15 years ago, Brillouin spectroscopy was applied to magnetostatic modes of ferromagnetic surfaces and films; some of the important experimental results and further references are given in Ref. 8. It may be expected that Brillouin spectroscopy will be applied to rare-earth surfaces and films; the typical frequency scale of 10–20 cm^{-1} in Figs. 3 and 5 is about an order of magnitude higher than that used in the work on ferromagnets, but it should be accessible to modern instruments. A quantitative theory of the Brillouin spectra requires, in the first instance, calculation of appropriate Green's functions in addition to mode frequencies. Furthermore, the modes observed in Brillouin scattering on ferromagnetics are often dipole exchange rather than pure dipolar. Extension of the present calculations to include exchange forces is possible in principle, but would require substantial effort.

The mode frequencies in Figs. 3 and 5 are intermediate between those for ferromagnetic and antiferromagnetic resonances. The difference between the latter is due to the fact that in ferromagnetic resonance the spin system precesses rigidly about the magnetic-field direction, whereas in antiferromagnetic resonance the relative direction of neighboring spins oscillates, and exchange forces come into play. For the spiral and cone states, the resonance frequencies also involve the exchange constants, as is seen from (30), although these are multiplied by trigonometric functions of the cone angles θ and ϕ. This gives a simple qualitative explanation for the intermediate-frequency range. Because of the higher δ frequency characteristic of antiferromagnets, it has been predicted[14] that the surface polaritons (retarded modes) on antiferromagnets should be observable by attenuated total reflection (ATR). The same is expected to hold for superlattices involving antiferromagnets.[15] The Fourier-transform spectrometers used nowadays in far-infrared ATR (Ref. 16) have an operating frequency range down to 10 cm^{-1} or a little less, and so magnetic polaritons on rare-earth magnets should be observable by this technique. Expressions for the surface-polariton dispersion curve and ATR reflectivity in terms of the susceptibility tensor are well known[8,15] and could be evaluated for the present case.

As mentioned in Sec. I, much of the current interest in rare-earth magnetism arises from the growth of superlattices involving rare earths. In addition to the alternation of different types of order, such as ferromagnetic with nonmagnetic or spiral with nonmagnetic, new ordering patterns can occur which are characteristic of the superlattice structure as a whole. Examples are the twisted state observed in Fe/Gd superlattices in parts of the H-T phase plane,[17] and the period-doubled state of Dy/Gd superlattices in which successive Dy spirals have opposite

helicity.[8] The present paper may be seen as a step toward the calculation of the rich spectrum of magnetostatic and retarded modes that my be expected in these various ordered states. For samples in which bulk-type ordering is present in layers which are thick on the atomic scale, it will be sufficient to characterize each layer by the corresponding bulk susceptibility. This is the analog of the bulk-slab model which has been applied extensively to semiconductor superlattices.[19] In fact, for the long wavelengths typical of the modes observed in Brillouin scattering and ATR, the effective-medium approximation[20–22] to the bulk-slab model may have an important part to play. This has proved very useful in interpreting ATR spectra of semiconductor superlattices;[23,24] the extension to magnetic superlattices[15,25,26] may be taken over for superlattices containing spiral or cone ordering in some layers without undue difficulty on the basis of the susceptibility expressions we have derived. For the more challenging situations where the ordering is specific to the superlattice itself, a microscopic calculation of the susceptibility is required, but it should be possible to base this on the techniques used in Secs. III and IV.

ACKNOWLEDGMENTS

N.S.A. thanks the Conselho Nacional de Desenvolvimento Científico e Tecnológico (CNPq) and the Royal Society for financial support to visit Essex, and D.R.T. thanks UFRN for financial support to visit Natal. The formulation of the problems discussed here benefitted greatly from discussions with R. E. Camley.

[1]B. R. Cooper, in *Solid State Physics,* edited by F. Seitz, D. Turnbull, and H. Ehrenreich (Academic, New York, 1968), Vol. 21, p. 393.
[2]R. J. Elliott, in *Magnetism,* edited by G. T. Rado and H. Suhl (Academic, New York, 1965), Vol. IIA, p. 385.
[3]T. Nagamiya, J. Appl. Phys. **33**, 1029 (1962).
[4]R. W. Damon and J. R. Eshbach, J. Phys. Chem. Solids, **19**, 308 (1961).
[5]L. K. Brundle and N. J. Freeman, Electron. Lett. **4**, 132 (1968).
[6]M. G. Cottam and D. J. Lockwood, *Light Scattering in Magnetic Solids* (Wiley, New York, 1986).
[7]R. E. Camley, Surf. Sci. Rep. **7**, 103 (1987).
[8]M. G. Cottam and D. R. Tilley, *Introduction to Surface and Superlattice Excitations* (Cambridge University Press, Cambridge, England, 1989).
[9]K. Mika and P. Grünberg, Phys. Rev. B **31**, 4465 (1985).
[10]A. Kueny, M. R. Khan, I. K Schuler, and M. Grimsditch, Phys. Rev. B **29**, 2879 (1984).
[11]U. Enz, Physica **26**, 698 (1960).
[12]T. A. Kaplan, Phys. Rev. **124**, 329 (1961).
[13]D. L. Mills in *Surface Excitations,* edited by V. M. Agranovich and R. Loudon (Elsevier, New York, 1984), Chap. 3.
[14]R. E. Camley and D. L. Mills, Phys. Rev. B **26**, 1280 (1982).
[15]N. S. Almeida and D. R. Tilley, Solid State Commun. **73**, 23 (1990).
[16]T. Dumelow and T. J. Parker, SPIE **1240**, 472 (1989).
[17]R. E. Camley and D. R. Tilley, Phys. Rev. B **37**, 3413 (1988).
[18]R. E. Camley, J. Kwo, M. Hong, and C. L. Chien, Phys. Rev. Lett. **64**, 2703 (1990).
[19]N. Raj and D. R. Tilley, in *The Dielectric Function,* edited by D. A. Khirznitz, L. V. Keldysh, and A. A. Maradudin (Elsevier, New York, 1989).
[20]V. M. Agranovich and V. E. Kravtsov, Solid State Commun. **55**, 85 (1985).
[21]N. Raj and D. R. Tilley, Solid State Commun. **55**, 373 (1985).
[22]W-M Liu, G. Eliasson, and J. J. Quinn, Solid State Commun. **55**, 533 (1985).
[23]T. Dumelow, A. R. El-Gohary, A. A. Hamilton, K. A. Maslin, T. J. Parker, N. Raj, B. Samson, S. R. P. Smith, D. R. Tilley, P. J. Dobson, C. T. B. Foxon, D. Hilton, and K. J. Moore, Mater. Sci. Eng. B **5**, 217 (1990).
[24]T. Dumelow, A. A. Hamilton, K. A. Maslin, T. J. Parker, B. Samson, S. R. P. Smith, D. R. Tilley, R. B. Beall, C. T. B. Foxon, J. J. Harris, D. Hilton, and K. J. Moore, in *Light Scattering from Semiconductor Superlattices,* edited by D. J. Lockwood and J. F. Young (Plenum, New York, 1991).
[25]N. Raj and D. R. Tilley, Phys. Rev. B **36**, 7003 (1987).
[26]N. S. Almeida and D. L. Mills, Phys. Rev. B **37**, 3400 (1988).